The Receptor Kinase IMPAIRED OOMYCETE SUSCEPTIBILITY1 Attenuates Abscisic Acid Responses in Arabidopsis[1][C][W]

Sophie Hok, Valérie Allasia, Emilie Andrio[2], Elodie Naessens, Elsa Ribes, Franck Panabières, Agnès Attard, Nicolas Ris, Mathilde Clément[3], Xavier Barlet, Yves Marco, Erwin Grill, Ruth Eichmann[4], Corina Weis, Ralph Hückelhoven, Alexandra Ammon, Jutta Ludwig-Müller, Lars M. Voll, and Harald Keller*

Institut Sophia Agrobiotech, Unité Mixte de Recherche 1355 Institut National de la Recherche Agronomique-Centre National de la Recherche Scientifique-Université Nice-Sophia Antipolis, 06903 Sophia Antipolis, France (S.H., V.A., E.A., E.N., E.R., F.P., Ag.A., N.R., H.K.); Unité Mixte de Recherche 6191 Commissariat à l'Energie Atomique, Centre National de la Recherche Scientifique, Laboratoire de Biologie du Développement des Plantes, Université d'Aix-Marseille, 13108 Saint-Paul-lez-Durance, France (M.C.); Laboratoire des Interactions Plantes Microorganismes, Unité Mixte de Recherche Centre National de la Recherche Scientifique-Institut National de la Recherche Agronomique 2594/441, 31326 Castanet-Tolosan, France (X.B., Y.M.); Technische Universität München, Lehrstuhl für Botanik (E.G.) and Lehrstuhl für Phytopathologie (R.E., C.W., R.H.), 85350 Freising-Weihenstephan, Germany; Institut für Botanik, Technische Universität Dresden, 01062 Dresden, Germany (J.L.-M.); and Friedrich-Alexander-Universität Erlangen-Nürnberg, Lehrstuhl für Biochemie, 91058 Erlangen, Germany (Al.A., L.M.V.)

In plants, membrane-bound receptor kinases are essential for developmental processes, immune responses to pathogens and the establishment of symbiosis. We previously identified the Arabidopsis (*Arabidopsis thaliana*) receptor kinase IMPAIRED OOMYCETE SUSCEPTIBILITY1 (IOS1) as required for successful infection with the downy mildew pathogen *Hyaloperonospora arabidopsidis*. We report here that IOS1 is also required for full susceptibility of Arabidopsis to unrelated (hemi)biotrophic filamentous oomycete and fungal pathogens. Impaired susceptibility in the absence of IOS1 appeared to be independent of plant defense mechanism. Instead, we found that *ios1-1* plants were hypersensitive to the plant hormone abscisic acid (ABA), displaying enhanced ABA-mediated inhibition of seed germination, root elongation, and stomatal opening. These findings suggest that IOS1 negatively regulates ABA signaling in Arabidopsis. The expression of ABA-sensitive *COLD REGULATED* and *RESISTANCE TO DESICCATION* genes was diminished in Arabidopsis during infection. This effect on ABA signaling was alleviated in the *ios1-1* mutant background. Accordingly, ABA-insensitive and ABA-hypersensitive mutants were more susceptible and resistant to oomycete infection, respectively, showing that the intensity of ABA signaling affects the outcome of downy mildew disease. Taken together, our findings suggest that filamentous (hemi)biotrophs attenuate ABA signaling in Arabidopsis during the infection process and that IOS1 participates in this pathogen-mediated reprogramming of the host.

[1] This work was supported by the French Laboratory of Excellence initiatives SIGNALIFE (grant no. ANR–11–LABX–0028–01) and TULIP (grant no. ANR–10–LABX–41), the French Plant Genomics program (grant no. ANR–08–GENM–137), the French Ministry for Education, Research, and Technology, and the German Research Foundation (grant nos. DFG FOR666 and DFG SFB924).

[2] Present address: Institut National de la Santé et de la Recherche Médicale, U1065, Centre Méditerranéen de Médecine Moléculaire, C3M, Toxines Microbiennes dans la Relation Hôte Pathogènes, 06204 cedex 3 Nice, France.

[3] Present address: Institut Sophia Agrobiotech, Unité Mixte de Recherche 1355 Institut National de la Recherche Agronomique-Centre National de la Recherche Scientifique-Université Nice-Sophia Antipolis, 06903 Sophia Antipolis, France.

[4] Present address: School of Life Sciences, University of Warwick, Gibbet Hill Campus, Coventry CV4 7AL, United Kingdom.

* Address correspondence to keller@sophia.inra.fr.

The author responsible for distribution of materials integral to the findings presented in this article in accordance with the policy described in the Instructions for Authors (www.plantphysiol.org) is: Harald Keller (keller@sophia.inra.fr).

[C] Some figures in this article are displayed in color online but in black and white in the print edition.

[W] The online version of this article contains Web-only data.

www.plantphysiol.org/cgi/doi/10.1104/pp.114.248518

Membrane-bound receptor-like kinases (RLKs) perceive molecules that mediate cell-to-cell communication during plant development, sense the biotic and abiotic environments, and transduce the perceived stimuli into complex downstream signaling networks. Hormones govern most of the essential events during vegetative and reproductive plant growth, and some RLKs are hormone receptors, integrating stress stimuli into adapted defense responses. The best-known examples are BRASSINOSTEROID INSENSITIVE1 and its co-RLK, BRASSINOSTEROID INSENSITIVE1-ASSOCIATED RECEPTOR KINASE1 (BAK1), which concertedly perceive brassinosteroid hormones. BAK1 also associates with pattern-recognition receptors that detect pathogens and induce innate immune responses (Chinchilla et al., 2009). Brassinosteroids tune these responses through synergistic and antagonistic effects on the immune signaling network triggered by the bacterial patterns recognized (Albrecht et al., 2012; Belkhadir et al., 2012). Another example involves PHYTOSULFOKINE RECEPTOR1 (PSKR1). Upon perception of the phytosulfokine hormone, PSKR1 modulates cellular dedifferentiation and

redifferentiation during organ development (Matsubayashi et al., 2002) but also integrates into the defense signaling network upon pathogen infection (Igarashi et al., 2012; Mosher et al., 2013). It was speculated that the principal function of PSKR1 signaling is to attenuate stress responses of cells during differentiation processes, such as vascularization (Motose et al., 2009). Concomitantly, PSKR1 affects the hormonal cross talk that regulates plant-pathogen interactions. RLKs also perceive cytokinins (Inoue et al., 2001) and ethylene (Hua and Meyerowitz, 1998). Other hormones, however, such as auxins (Tan et al., 2007), GAs (Ueguchi-Tanaka et al., 2005), and abscisic acid (ABA), interact with intracellular rather than membrane-bound receptors. ABA recognition at the membrane has been discussed (Liu et al., 2007), but it is now well established that the hormone binds to PYRABACTIN RESISTANCE (PYR)/PYRABACTIN RESISTANCE1-LIKE (PYL)/REGULATORY COMPONENT OF ABSCISIC ACID RECEPTOR (RCAR), leading to the formation of stable complexes with type 2C protein phosphatases (PP2Cs) and to their subsequent inhibition (for review, see Cutler et al., 2010). These complexes form the early ABA signaling module, which interacts with ion channels, transcription factors, and other targets, providing a mechanistic connection between the phytohormone and ABA-induced responses. ABA responses are fine-tuned through a network of regulators including membrane receptors that sense developmental processes and environmental conditions. Examples include FERONIA (FER; Yu et al., 2012), A4 lectin receptor kinases (Xin et al., 2009), and CYSTEINE-RICH RECEPTOR-LIKE KINASE36 (CRK36; Tanaka et al., 2012), all of which down-regulate ABA signaling. Other sensors of environmental stress, such as PROLINE-RICH EXTENSIN-LIKE RECEPTOR KINASE4 (Bai et al., 2009) and RECEPTOR-LIKE PROTEIN KINASE1 (Osakabe et al., 2005), act in the opposite direction, up-regulating ABA signaling. ABA signaling modulates pathogenesis in diverse plant-pathogen interactions and is involved in the cross talk with plant defense pathways (Robert-Seilaniantz et al., 2011).

We previously identified the RLK IMPAIRED OOMYCETE SUSCEPTIBILITY1 (IOS1; At1g51800) as required for the full susceptibility of Arabidopsis (*Arabidopsis thaliana*) to the downy mildew pathogen *Hyaloperonospora arabidopsidis* (*Hpa*; Hok et al., 2011). IOS1 belongs to a subfamily of approximately 50 RLKs in Arabidopsis, which possess an extracellular region composed of a malectin-like domain (MLD) in addition to (two to three) leucine-rich repeats (LRRs; Hok et al., 2011). Malectin was first identified in *Xenopus laevis* as an endoplasmic reticulum-localized carbohydrate-binding protein (Schallus et al., 2008) that controls the *N*-glycosylation status of secreted glycoproteins (Chen et al., 2011). The role of MLDs in plants, notably as elements of the extracellular region of RLKs, is yet unknown (Lindner et al., 2012). The protein sequence and domain organization of IOS1 have strong similarities with the SYMBIOSIS RECEPTOR-LIKE KINASE (SYMRK) and SYMRK-like RLKs from legumes, which are key regulators of the accommodation of fungal and bacterial symbionts (Stracke et al., 2002; Capoen et al., 2005; Markmann et al., 2008). Similar to SYMRK, IOS1 contains the conserved sequence GDPC within the interspace between MLD and LRRs of the extracellular domain (Hok et al., 2011). This motif is required for establishing the epidermal symbiotic program in roots but not the subsequent cortical symbiosis, suggesting the perception of distinct signals by the extracellular domain of SYMRK during the compatible plant-microbe interaction (Kosuta et al., 2011). IOS1 was recently shown to form a complex with the pattern recognition receptors FLAGELLIN SENSING2 (FLS2) and EF-TU RECEPTOR (EFR), as well as with BAK1, and to prime pattern-triggered immunity (PTI) to the bacterium *Pseudomonas syringae* (Chen et al., 2014). However, during the interaction of Arabidopsis with *Hpa*, IOS1 supports the success of downy mildew infection rather than PTI (Hok et al., 2011). The physiological programs that are regulated by IOS1 in this interaction are yet unknown.

Here, we investigated the function of IOS1 during the interaction with *Hpa* and unrelated filamentous biotrophic and hemibiotrophic pathogens. Collectively, our results show that IOS1 down-regulates ABA responses, thereby creating an environment that favors the biotrophic lifestyle of these pathogens.

RESULTS

IOS1 Promotes Infection by Filamentous (Hemi)Biotrophs

The transcription of *IOS1* was activated by the infection of cotyledons with *Hpa* (Hok et al., 2011). This activation occurred locally at the early appressorium-mediated penetration stages of infection (Fig. 1A) in the single-cell layers surrounding the invading hyphae, which harbor haustoria (Fig. 1B). We further analyzed whether infection-responsive transcription of the *IOS1* gene was restricted to leaf tissues by inoculating Arabidopsis roots with the hemibiotrophic oomycete pathogen *Phytophthora parasitica*. In noninoculated roots of the *IOS1* reporter line, *IOS1* expression was only observed in the elongation zone but not in the root tip (Fig. 1C). Upon inoculation, *P. parasitica* zoospores attach to the root tip, penetrate the root via an appressorium, grow toward the central cylinder, and invade the roots and aerial organs (Attard et al., 2010). The transcription of IOS1 was activated during the initial biotrophic phase of *P. parasitica* invasion (Fig. 1C), and the development of disease was significantly delayed in the *ios1-1* loss-of-function mutant (Fig. 1D). The activation of *IOS1* transcription by both leaf and root oomycete pathogens thus appears to be required for successful infection. A similar observation was made with the unrelated powdery mildew fungus *Erysiphe cruciferarum*. On Arabidopsis leaves, germinating *E. cruciferarum* conidia develop appressoria, which produce penetration pegs and haustoria within leaf epidermal cells, while the fungal mycelium grows on the leaf surface. During *E. cruciferarum* infection, *IOS1* transcription was activated in the mesophyll cells underlying the epidermal infection sites (Supplemental Fig. S1A).

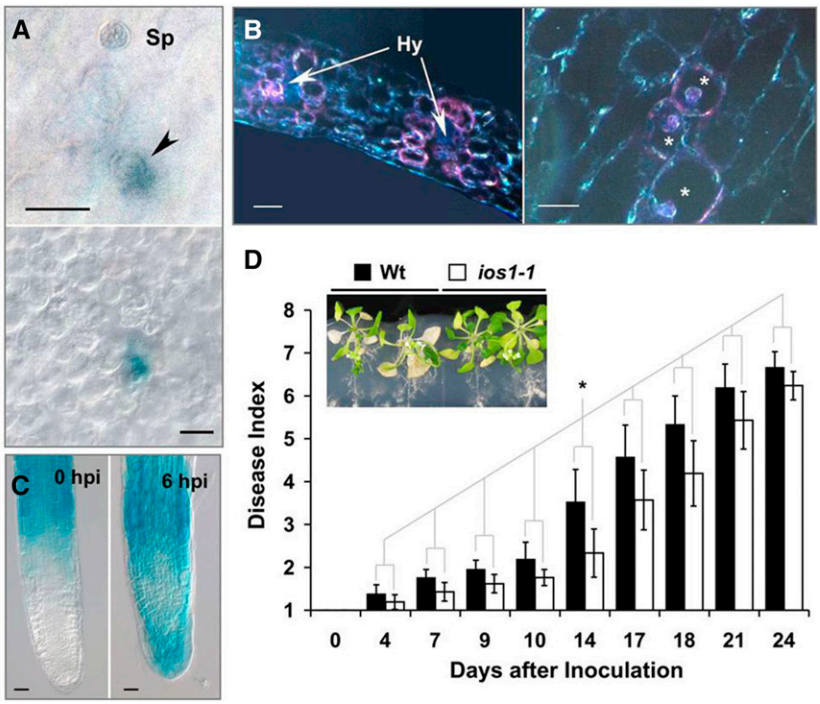

Figure 1. The *ios1-1* mutation impairs susceptibility to filamentous (hemi)biotrophs. A, Transcriptional activation of *IOS1* by *Hpa*, as analyzed by transmission light microscopy for GUS activity (blue), 4 h after inoculation of the previously described *IOS1* reporter line (Hok et al., 2011). Nongerminated spores (Sp) and spores penetrating from an appressorium (arrowhead) are visibly attached to cotyledon surfaces (top). GUS staining is localized to the mesophyll cells underlying the penetration site (bottom; with a different optic focus). B, Transcriptional activation of *IOS1* by *Hpa*, as analyzed by dark-field microscopy of thin sections of cotyledons from the reporter line, 3 d after inoculation. GUS activity is shown in red. Cross sections (left) and tangential sections (right) reveal localized GUS activity in single-cell layers around invading hyphae (Hy) harboring haustoria (asterisks). C, Transcriptional activation of *IOS1* by *P. parasitica*, as shown by transmission light micrographs of *IOS1* reporter activity in root tips. In the absence of infection, *IOS1* is expressed in elongation zones only (left; compare with Fig. 3). Inoculation with *P. parasitica* zoospores activates the *IOS1* promoter during the initial biotrophic phase, in which hyphae invade cells from the root cap and the differentiation zone, and 6 h after inoculation (hpi; right). D, *P. parasitica* disease is delayed in the *ios1-1* mutant. The photograph shows representative wild-type (Wt; left) and mutant (right) plants at 18 d after inoculation. The development of disease in wild-type and *ios1-1* plants was assessed on the basis of an established score (Attard et al., 2010). The means and 95% two-tailed confidence intervals are shown. Differences in disease development between wild-type and *ios1-1* plants were statistically significant (asterisk), as demonstrated by Scheirer-Ray-Hare nonparametric two-way ANOVA for ranked data ($P = 0.00186$).

IOS1 expression in the mesophyll appeared to favor the progression of disease, as inoculated plants from the *ios1-1* mutant line exhibited fewer powdery mildew symptoms on leaves than wild-type plants (Supplemental Fig. S1B). Accordingly, significantly fewer conidiophores were produced on the *ios1-1* mutant than on the wild type (Supplemental Fig. S1C). The observed interaction phenotypes with mildews are not caused by growth defects of the mutant, as the vegetative development of *ios1-1* was indistinguishable from that of the wild type (Supplemental Fig. S2). Wild-type and mutant plants were equally susceptible to root inoculations with the wilt bacterium *Ralstonia solanacearum* (Supplemental Fig. S1D), indicating that the development of bacterial wilt occurs independently of IOS1. Taken together, our findings suggest that the host receptor IOS1 contributes to successful leaf and root invasions by filamentous (hemi)biotrophs.

Absence of IOS1 Does Not Strengthen Defense Responses

The interaction phenotypes of the *ios1-1* mutant might be the consequence of either a loss of susceptibility or a gain of resistance. We thus analyzed whether the mutation of *IOS1* led to increases in the activation of defense signaling pathways and immune responses. We used reverse transcription-quantitative polymerase chain reaction (RT-qPCR) to determine the expression of a set of genes that were previously described as being up-regulated upon the onset of defense signaling. These genes code for FLAGELLIN22 (FLG22)-INDUCED RECEPTOR-LIKE KINASE1 (FRK1), NON-RACE-SPECIFIC DISEASE RESISTANCE1/HAIRPIN-INDUCED1-LIKE10 (NHL10), PHYTOALEXIN DEFICIENT4 (PAD4), and the transcription factors WRKY29, WRKY33, and WRKY70 (characterized by the conserved amino acid sequence WRKY). FRK1, NHL1, and WRKY29 are key components of PTI signaling pathways, and the genes encoding them

are expressed at early time points upon the perception of pathogen-associated molecular patterns (Asai et al., 2002; He et al., 2006; Boudsocq et al., 2010). We did not detect statistically significant differences ($P > 0.05$) in the expression of *FRK1*, *NHL10*, and *WRKY29* between *Hpa*-infected wild-type and *ios1-1* plants (Fig. 2, A and B). The expression of *FRK1* follows the initial transient profile, which was previously reported for a compatible interaction with *P. syringae* (He et al., 2006), and is then up-regulated at later time points of *Hpa* infection in both the wild type and the mutant (Fig. 2A). Minor but significant differences ($P < 0.05$) between wild-type and *ios1-1* plants were detectable in the transcriptional activation of *PAD4*, *WRKY33*, and *WRKY70* (Fig. 2, A and B). An up-regulation of these genes was observed during the early time points of interaction at 8 to 24 h after inoculation. PAD4 is a central regulator in the generation of downstream disease resistance responses following effector-activated TOLL/INTERLEUKIN1 RECEPTOR-NUCLEOTIDE-BINDING-LRR proteins and is involved in salicylic acid (SA)-mediated signal transduction (Wiermer et al., 2005). WRKY33 integrates jasmonic acid (JA)- and ethylene-dependent defense pathways (Birkenbihl et al., 2012; Meng et al., 2013), whereas WRKY70 acts as a node of convergence for SA- and JA-dependent signaling events (Li et al., 2006). Therefore, we analyzed whether the mild increases in *PAD4*, *WRKY33*, and *WRKY70* expression affect the balance between SA-, JA-, and ethylene-dependent signaling in the mutant. To this end, we determined the influence of IOS1 on the transcriptional activation of SA, JA, and ethylene target genes in response to *Hpa* infection. The expression of *PATHOGENESIS-RELATED 1a* (*PR1a*) reflects the activation of SA-mediated responses, whereas *PLANT DEFENSIN1.2* (*PDF1.2*) and *PR4* are marker genes for the JA- and ethylene-mediated defense signaling pathway in Arabidopsis (Robert-Seilaniantz et al., 2011). During *Hpa* infection, SA-dependent responses are the most effective, while JA and ethylene-dependent responses do not generally

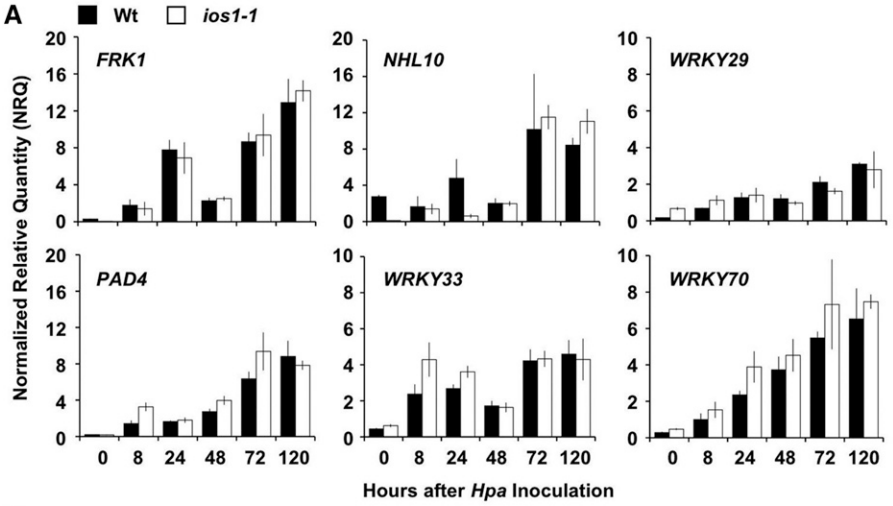

B

Gene	Mutant vs. Wt (Genotype)	Inoculation Period (Time)	Genotype x Time	Gene	Mutant vs. Wt (Genotype)	Inoculation Period (Time)	Genotype x Time
FRK1	0.466	$< 10^{-12}$ ***	0.969	*PAD4*	0.024 *	$< 10^{-12}$ ***	0.105
NHL10	0.416	$< 10^{-3}$ ***	0.934	*WRKY33*	0.012 *	$< 10^{-4}$ ***	0.010 *
WRKY29	0.712	0.008 **	0.425	*WRKY70*	0.025 *	$< 10^{-7}$ ***	0.792

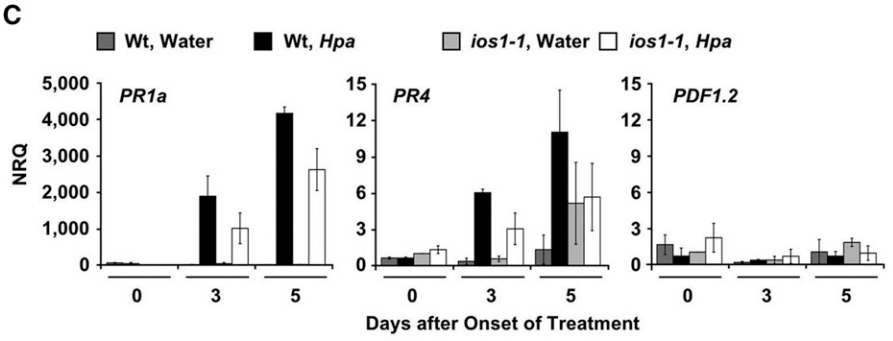

Figure 2. Impaired *ios1-1* susceptibility is unlikely to result from up-regulated defense. A, Expression profile of genes coding for immune signaling elements in Arabidopsis. RT-qPCR analyses were performed with seedlings from *Hpa*-infected wild-type (Wt) and *ios1-1* mutant plants over a time course of 5 d after inoculation. The data shown are means and SD of three biological replicates. B, Summary of the *P* values associated with the statistical analysis of the data presented in A. For each gene, two factors (genotype and time) were treated as fixed (model I of three-way ANOVA) and crossed. For each of the 30 tested individual situations (two genotypes × five time points × three biological replicates), the mean expression of a technical triplicate was taken into account, assuming a Gaussian distribution and the homoscedasticity. Analysis was performed using the software R (http://www.r-project.org/). *$0.05 > P > 0.01$, **$0.01 > P > 0.001$, ***$P < 0.001$. C, RT-qPCR analysis for the expression of genes coding for PR proteins and a plant defensin in noninoculated and *Hpa*-infected plants from the wild type and the *ios1-1* mutant. Neither SA- nor JA/ethylene-mediated defense responses were up-regulated in the *ios1-1* mutant. The data shown are means and SD of two independent biological replicates. NRQ, Normalized relative quantities.

play a major role in defense against downy mildew (Glazebrook, 2005). Accordingly, we found a strong induction of *PR1a* expression upon *Hpa* infection, whereas *PR1a* transcripts were nearly absent from water-treated controls. The observed induction by *Hpa* was not enhanced in the *ios1-1* background but rather reduced, likely due to the lower infection density in the mutant (Fig. 2C). Pathogen-responsive transcriptional activation of *PR4* and *PDF1.2* occurred to much lower levels than *PR1a*, and significant increases in the mutant background were not detected, when compared with the wild type (cutoff, $P < 0.05$). Similar to *PR1a*, infection-responsive expression of *PR4* was lower in *ios1-1* (Fig. 2C) than in the wild type.

We then analyzed whether the reduced susceptibility of *ios1-1* to *E. cruciferarum* was accompanied by increases in callose deposition. The amount and extent of callose reflect the defense response of Arabidopsis toward the powdery mildew fungus (Ellinger et al., 2013). We found no obvious differences between the wild type and the mutant, and we could not observe an increased number or size of callose deposits around *E. cruciferarum* penetration sites in the *ios1-1* mutant (Supplemental Fig. S3).

Although we cannot exclude that subtle changes in immune signaling pathways are caused by the *ios1-1* mutation, we conclude from our data that the reduced susceptibility of *ios1-1* is unlikely to result from enhanced defense activation; rather, it is due to the lack of a host function, which is required for successful infection.

Absence of IOS1 Confers Hypersensitivity to ABA

To gather more information on the physiological function of IOS1, we investigated its expression during the Arabidopsis life cycle. We observed tissue-specific *IOS1* expression in the radicle emerging from the testa, in the elongation zones of roots, and in root cap border cells undergoing detachment (Fig. 3, A–E). In hypocotyls, *IOS1* expression was detected only during etiolation in the dark (Fig. 3, F and G). In cotyledons and leaves, expression was restricted to cells surrounding stomata (Fig. 3H). In reproductive organs, *IOS1* expression was observed in the style after pollination, in the abscission zones of sepals and petals, in the transmitting tract of developing fruits, and in the abscission zones of mature siliques (Fig. 3, I–O). In summary, *IOS1* was predominantly expressed in tissue with fates controlled by the phytohormone ABA. However, exogenous ABA application to leaves did not activate the *IOS1* promoter (Supplemental Fig. S4A), and the elimination of ABA from roots with an inhibitor of carotenoid synthesis did not impair *IOS1* expression (Supplemental Fig. S4, B and C). IOS1 expression, therefore, is not upregulated by ABA.

Based on the *IOS1* expression profile, we investigated the possible involvement of the receptor kinase in ABA signaling. Exogenous ABA application to seeds and seedlings inhibits seed germination and cell elongation, respectively. We found that *ios1-1* mutant plants were significantly more sensitive to ABA-induced inhibition of both seed germination (Fig. 4A) and primary root elongation (Fig. 4B) when compared with wild-type plants and the complemented mutant line *ios1-1cp4*. ABA also modulates stomatal aperture and regulates foliar transpiration, thus influencing the leaf surface temperature. We investigated the effect of IOS1 on stomatal aperture by subjecting leaves from wild-type and mutant plants to thermographic measurements (Jones, 1999). We found that the rosette leaf temperatures of *ios1-1* were significantly higher under continuous light than those of the wild type but similar to those of the ABA-hypersensitive *abh1* mutant (Hugouvieux et al., 2001; Fig. 4C). Since we could not distinguish the *ios1-1* mutant from the wild type in terms of stomata morphology or density (Fig. 4D), we concluded that the higher leaf surface temperature of *ios1-1* resulted from limited pore aperture. The transition from darkness to light induces stomatal opening, which is inhibited by ABA (Mustilli et al., 2002). By contrast, the treatment of epidermal strips with the ATP-sensitive potassium channel inhibitor glibenclamide leads to the concerted inhibition of outward Cl^- and K^+ channels in guard cells, inducing stomatal opening even in the dark (Leonhardt et al., 1999). We measured stomatal pore width on epidermal strips from wild-type and mutant leaves treated with water or ABA in the dark before exposure to light. Alternatively, epidermal strips were treated with water and glibenclamide in the dark and were then further incubated in the dark. We observed that ABA inhibited stomatal opening in the light by about 0.5 μm on epidermal strips from wild-type plants but by about 2.5 μm on those from the *ios1-1* mutant. Stomatal opening, therefore, was more sensitive to ABA in the mutant than in the wild type. Glibenclamide treatment induced stomatal opening in the dark by about 1 μm in both the wild type and the mutant (Fig. 4E), suggesting that the *ios1-1* mutation had no effect on ABA-responsive ion channels. We then compared the stomatal conductance of leaves in response to different ABA concentrations. In the absence of ABA, stomatal conductance did not differ significantly between mutant and wild-type plants under our experimental conditions. Increasing ABA concentrations decreased conductance in all lines (Fig. 4F). This effect was significantly stronger in the *ios1-1* mutant than in the wild type or the *ios1-1cp4* line. Taken together, our findings show that a loss of IOS1 confers ABA hypersensitivity to Arabidopsis.

ABA Signaling Interferes with Infection by Downy Mildew and Is Attenuated by IOS1

We analyzed the ABA contents in noninoculated and *Hpa*-infected cotyledons from wild-type plants, the *ios1-1* mutant, and the complemented mutant *ios1-1cp4* and did not find significant differences in ABA

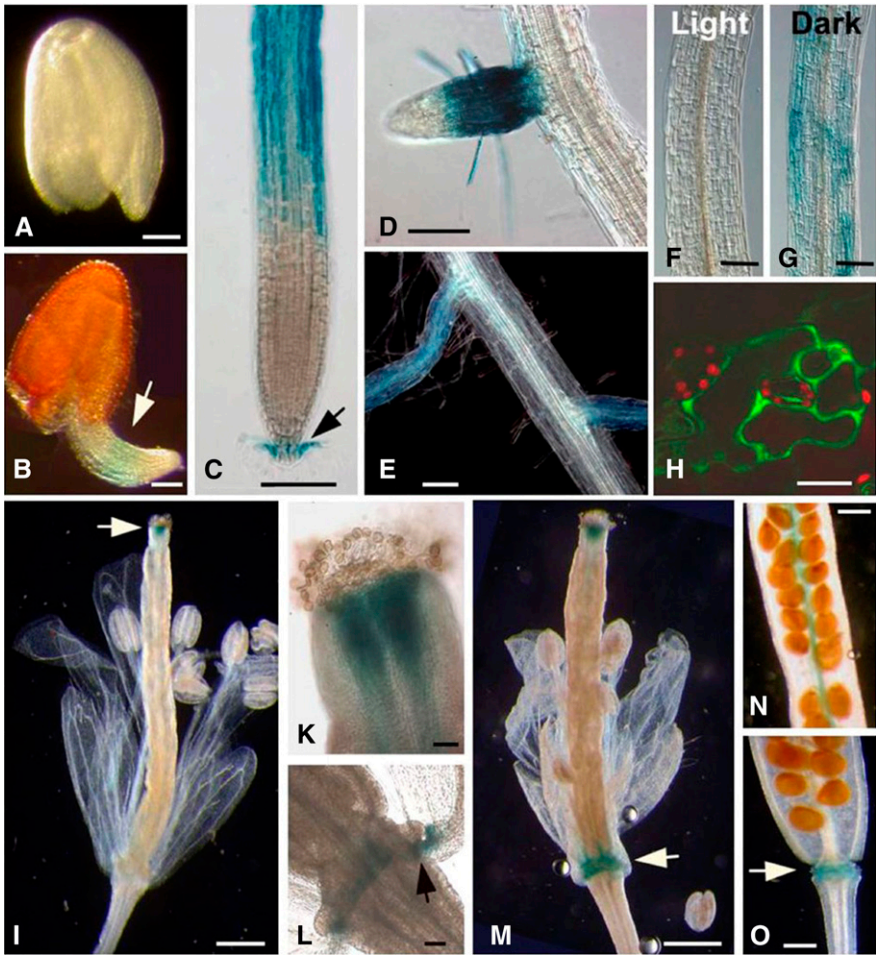

Figure 3. Tissue specificity of *IOS1* expression in Arabidopsis organs at different developmental stages. The transcriptional activation of *IOS1* in vivo is revealed either by enzymatic GUS activity (blue) or by GFP fluorescence in transgenic lines carrying the *pIOS1*::*GFP-GUS* reporter gene construct. A to H, *IOS1* expression during vegetative growth. I to O, *IOS1* expression during reproduction. Reporter activity is not detectable in the embryo (A) but can be seen in the radicle emerging from the testa (B), indicating transcriptional *IOS1* activation in the elongation zone (arrow). In primary roots, GUS activity is limited to the elongation zone (C) and to root cap border cells undergoing detachment (arrow). The *GUS* reporter gene is not transcribed in fully expanded root cells (D and E), but the transcription of this gene is reinitiated in emerging (D) and elongating (E) secondary roots. In hypocotyls, GUS activity is detected only during etiolation, in the dark (G), with no activity detected in nonetiolated tissues in the light (F). In cotyledons and leaves, *IOS1* expression is restricted to the cells surrounding the stomata, as shown by confocal microscopy of the GFP reporter (H). GFP appears in green, and red spots represent chloroplasts within stomatal guard cells. GUS activity is observed after pollination, in the style (I; arrow), corresponding to the development of pollen tubes (K). During the subsequent development of the pollinated flowers, *IOS1* activation occurs in the abscission zones of sepals and petals (L and M; arrows), in the transmitting tract of developing fruits (N), and, finally, in the abscission zones of mature siliques (O; arrow). Bars = 10 μm (H), 50 μm (F and G), 100 μm (A–E, K, and L), and 500 μm (I and M–O).

levels between genotypes (Supplemental Fig. S5). These data suggest that IOS1 interferes with ABA signaling or the onset of responses, rather than with the accumulation of the hormone, and that the ABA hypersensitivity of *ios1-1* derives from the absence of a negative regulatory element in ABA signaling. We thus analyzed the transcriptional induction of genes coding for COLD REGULATED (COR) and RESISTANCE TO DESICCATION (RD) proteins in cotyledons from wild-type and *ios1-1* mutant plants at different time points after water treatment or *Hpa* inoculation. The transcriptional up-regulation of *COR* and *RD* genes conventionally reflects activated ABA signaling in Arabidopsis (Guo et al., 2002). We found that *COR15A*, *COR15B*, and *RD29A* were transiently activated in the control situation (i.e. in water-treated cotyledons of plants that were grown at 20°C and transferred to the inoculation temperature of 16°C). Transcription of these genes was enhanced in *ios1-1* at all time points, thus confirming the ABA hypersensitivity of the mutant, and reduced upon inoculation with *Hpa* in both genotypes (Fig. 5A). The reduction in *COR/RD* gene expression upon infection was less pronounced in *ios1-1* than in the wild type, particularly during the first day of infection. We found

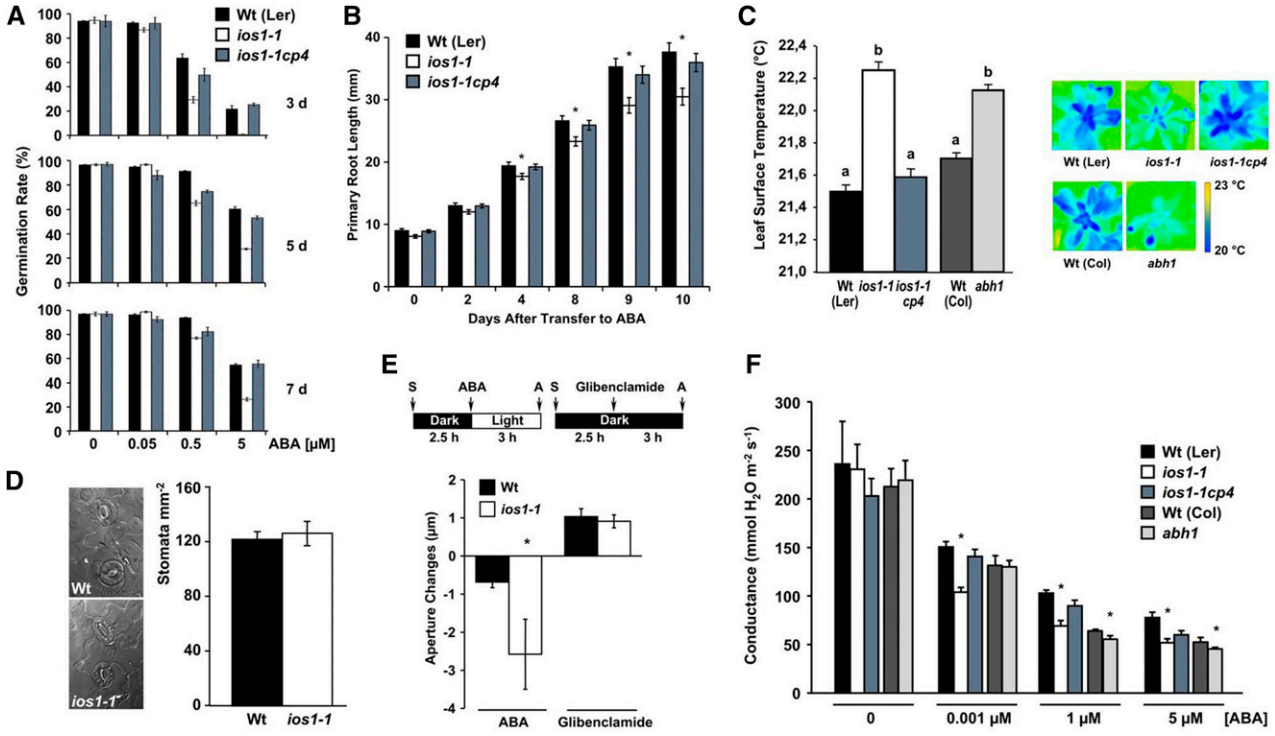

Figure 4. The *ios1-1* mutant is ABA hypersensitive. A, Seed germination on medium containing ABA is more strongly inhibited in *ios1-1* seeds than in both the wild type (Wt; L*er*, Landsberg *erecta*) and the complemented mutant line *ios1-1cp4* (Hok et al., 2011). Values shown are means and SD for radicle emergence rates determined for three plates, each containing about 100 seeds, for line, and for (±)-ABA concentration. B, The *ios1-1* mutant is more sensitive to the ABA-induced inhibition of primary root elongation. Seven-day-old plantlets were transferred to medium containing or not 10 μM (±)-ABA, and primary root elongation was measured 2, 4, 8, 9, and 10 d later. Shown are means and SE of 30 individual plants per line. Without ABA, wild-type, *ios1-1*, and complemented mutant plants attained similar mean primary root lengths of 73.4 ± 2.1, 73.1 ± 2, and 71.4 ± 1.5 mm, respectively, 10 d after transfer. C, Leaf surface temperature is higher in the *ios1-1* mutant than in the wild type. Elevated leaf temperatures of *ios1-1* were similar to those of the *abh1* mutant (background Columbia [Col]). Shown are thermographs of a representative plant from each line and the means and SD of 20 measured replicates of eight plants per line, which were obtained 48 h after exposure of the plants to continuous light. The significance of differences was determined in Student's *t* test (identical letters, not significantly different with $P > 0.01$; different letters, $P < 0.01$). D, Stomatal development is not affected in the *ios1-1* mutant. The micrographs illustrate representative, fully developed stomata on epidermal strips from rosette leaves of wild-type and mutant plants. The graph shows the mean stomatal density and SD of four independent experiments. E, The *ios1-1* mutant is hypersensitive to the ABA-regulated inhibition of stomatal opening, but its ion channel-mediated stomatal movement appears normal. Plants were treated as indicated in the sketch above the graph. Values shown are mean aperture changes and SD of 70 stomata on treated strips, based on the apertures of the same number of stomata from untreated controls from mutant and wild-type plants. The beginning (S [for start]) and end (A [for analysis]) of the experimental onsets are indicated. F, Stomatal conductance in response to various concentrations of ABA (in μM). Values indicate means and SD of measurements of at least five plants per line and per treatment. Specific treatments of leaves prior to measurements are indicated in "Materials and Methods." Asterisks in A, B, and E indicate significant differences, with $P < 0.01$, as determined in Student's *t* test. Asterisks in F indicate significant differences, with $P < 0.05$, as determined by a modified Welch-Satterthwaite test implemented in the VANTED software package. [See online article for color version of this figure.]

that *COR15A* and *COR15B* were transiently induced upon exogenous application of ABA to cotyledons and that transcript accumulation peaked around 2 to 4 h after spray treatment of the wild type or of *ios1-1cp4*. In ABA-treated *ios1-1* mutant plants, a maximum of *COR* gene transcripts accumulated already 1 h after ABA application (Supplemental Fig. S6). IOS1 thus appears to interfere with the timing of ABA signaling rather than with its amplitude.

Among the *COR/RD* marker genes that were analyzed by RT-qPCR for infection-related regulation in the absence or presence of IOS1, we found weak differences in *RD29B* transcript levels. We thus used an experimental approach that allowed measuring the cumulative, ABA-dependent transcriptional activation of this gene over 3 d of treatment. We generated *ios1-1* mutant and wild-type lines harboring a fusion between the *RD29B* promoter (Christmann et al., 2005) and the β-D-glucuronidase (*gusA*) gene (Jefferson et al., 1987), which allowed us to measure the activity of the stable GUS reporter as a readout for in planta and in vitro studies. We stimulated ABA signaling in water-treated

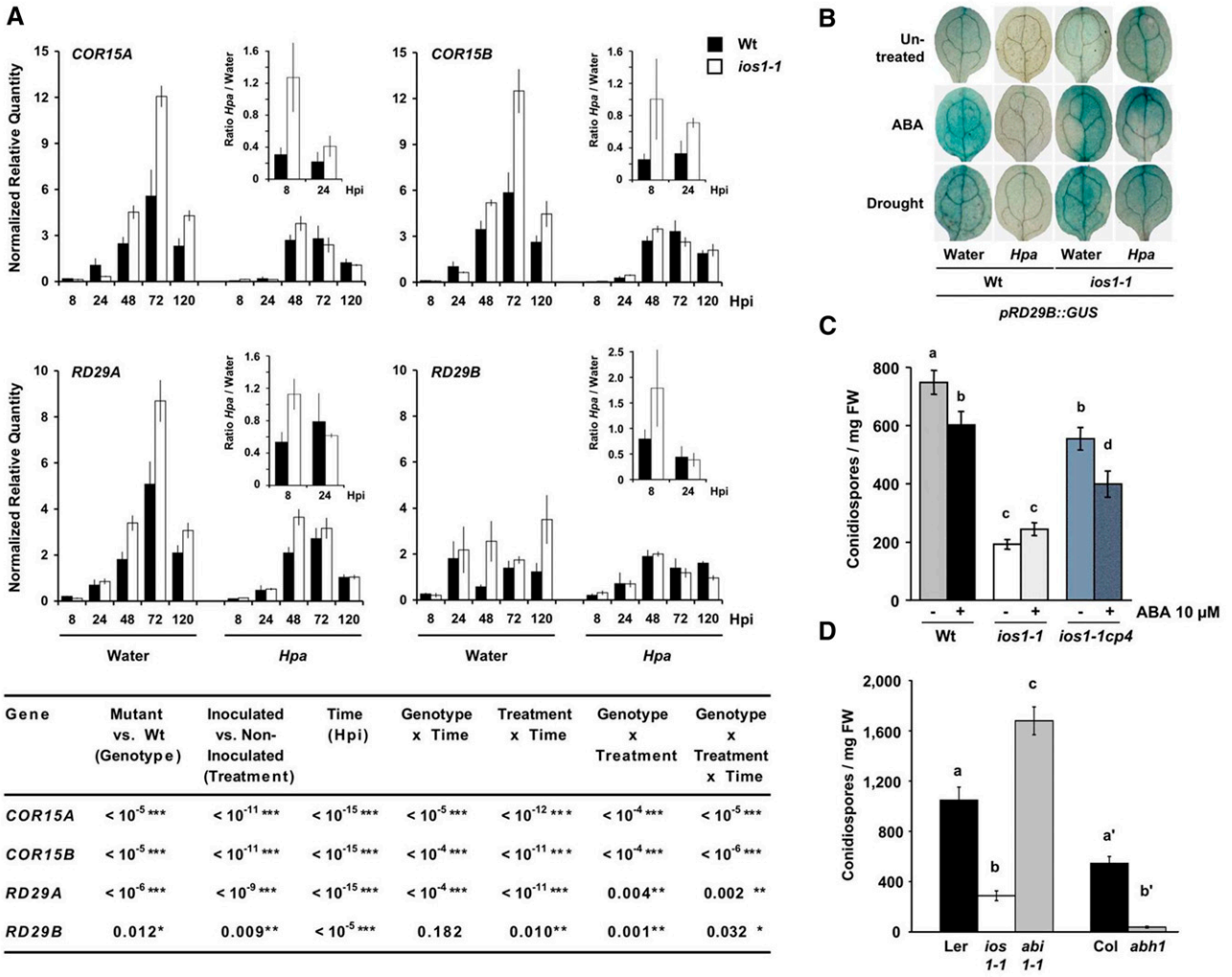

Gene	Mutant vs. Wt (Genotype)	Inoculated vs. Non-Inoculated (Treatment)	Time (Hpi)	Genotype x Time	Treatment x Time	Genotype x Treatment	Genotype x Treatment x Time
COR15A	$< 10^{-5}$ ***	$< 10^{-11}$ ***	$< 10^{-15}$ ***	$< 10^{-5}$ ***	$< 10^{-12}$ ***	$< 10^{-4}$ ***	$< 10^{-5}$ ***
COR15B	$< 10^{-5}$ ***	$< 10^{-11}$ ***	$< 10^{-15}$ ***	$< 10^{-4}$ ***	$< 10^{-11}$ ***	$< 10^{-4}$ ***	$< 10^{-6}$ ***
RD29A	$< 10^{-6}$ ***	$< 10^{-9}$ ***	$< 10^{-15}$ ***	$< 10^{-4}$ ***	$< 10^{-11}$ ***	0.004**	0.002 **
RD29B	0.012*	0.009**	$< 10^{-5}$ ***	0.182	0.010**	0.001**	0.032 *

Figure 5. ABA signaling interfering with disease is attenuated by IOS1. A, RT-qPCR experiments to determine the time course of ABA-regulated *COR15A/B* and *RD29A/B* marker gene transcript levels in *Hpa*-infected and noninfected wild-type (Wt) and *ios1-1* plants. Represented are means and SD of normalized relative quantities, which were obtained for samples from three independent biological replicates. The insets represent the mean normalized relative quantity ratios and SD between inoculated and non-inoculated plants from the same genotype at 8 and 24 h after inoculation (Hpi). The table below the graphs summarizes the *P* values that were associated with the statistical analysis of the data. For each gene, three factors (genotype, treatment, and time) were treated as fixed (model I of three-way ANOVA) and crossed. For each of the 60 tested individual situations (two genotypes × two treatments × five time points × three biological replicates), the mean expression of a technical triplicate was taken into account. Analysis was performed using the software R. *$0.05 > P > 0.01$, **$0.01 > P > 0.001$, ***$P < 0.001$. B, Representative cotyledons from the wild type (left) and the *ios1-1* mutant (right) harboring the *pRD29B::GUS* construct 3 d after control treatment (water) or after inoculation with *Hpa*. ABA signaling and reporter gene expression were either not particularly induced (Untreated) or stimulated by spraying ABA onto cotyledons (ABA) or by lowering relative humidity (Drought). For a compiled view of the experiment and for quantitative analyses, see Supplemental Figure S7. C, Exogenous application of ABA (10 μM) decreases the reproduction *of Hpa* on the wild type and the complemented *ios1-1* mutant (*ios1-1cp4*). It does not further decrease the lowered susceptibility of *ios1-1*. D, ABA signaling interferes with *Hpa* infection. The Landsberg *erecta* (Ler) wild type and mutants in this background (*abi1-1* and *ios1-1*) were inoculated with the compatible *Hpa* isolate Wela. The Columbia (Col) wild type and the *abh1* mutant were inoculated with the compatible isolate Noco2. The values shown in C and D are means and SE of 20 replicates. The significance of differences was determined in Student's *t* test (different letters, $P < 0.001$). FW, Fresh weight.

and *Hpa*-infected cotyledons, either by applying ABA or by lowering relative humidity to stimulate drought responses (Uno et al., 2000). Both treatments enhanced *RD29B* promoter activity and stimulated synthesis of the GUS reporter protein in uninfected cotyledons from both wild-type and *ios1-1* plants. Reporter activity was substantially reduced in *Hpa*-infected cotyledons of the wild type but not in *Hpa*-infected cotyledons of the *ios1-1* mutant (Fig. 5B; Supplemental Fig. S7). To obtain quantitative data, we measured GUS activity under the different experimental conditions. In the wild-type background, infection with *Hpa* decreased GUS by up

to 60%. No down-regulation of ABA-sensitive reporter gene expression occurred in the *ios1-1* mutant background, and GUS activity was comparable in the presence and absence of infection (Supplemental Fig. S7B).

Our findings suggest that IOS1 down-regulates ABA signaling, thereby promoting disease progression in downy mildew-infected tissue (Supplemental Fig. S8). This implies that ABA signaling impedes the infection process and that its down-regulation promotes disease. Consistent with this hypothesis, we found that exogenous ABA application to cotyledons significantly interfered with downy mildew disease on the wild type and the complemented mutant, whereas it did not further reduce sporulation on *ios1-1* (Fig. 5C). In further support of this hypothesis, we noted that ABA-insensitive (*abi1-1*; Koornneef et al., 1984) and ABA-hypersensitive (*abh1*) signaling mutants were significantly more susceptible and more resistant to *Hpa* infection, respectively (Fig. 5D).

DISCUSSION AND CONCLUSION

Our findings identify IOS1 as a novel element in the network regulating ABA responses. *IOS1* expression is specific to particular tissues or developmental stages exhibiting a tight control of ABA responses (Fig. 3) and becomes induced in response to infection with filamentous, hemibiotrophic, or biotrophic pathogens (Fig. 1). Our data thus suggest that these pathogens benefit from the IOS1-mediated down-regulation of ABA signaling to accomplish their infection cycle. The role of ABA in plant-microbe interactions is ambiguous but seems to be dependent on the lifestyle of infecting pathogens, the plant tissue, and the time point of infection (Ton et al., 2009). The Arabidopsis *abi1-1* ABA signaling mutant was previously shown to be susceptible to *Hpa* but more resistant to *P. syringae*, thus indicating that ABA signaling promotes the multiplication of the bacterium but not the development of *Hpa* in plant tissues (Mohr and Cahill, 2003). We show that susceptibility to downy mildew is increased in cotyledons of the signaling mutant *abi1-1*, supporting that *P. syringae* and *Hpa* require ABA signaling in Arabidopsis in an opposite manner during the initial infection process. Consistent with this, we found the ABA-hypersensitive mutant *abh1* more resistant to *Hpa* infection, whereas the opposite effect was observed when this mutant interacted with *P. syringae* (de Torres-Zabala et al., 2007). Since our data show that neither the *IOS1* genotype nor *Hpa* infection had an influence on ABA levels in cotyledons (Supplemental Fig. S5), we conclude that IOS1 interferes with ABA signaling rather than with its accumulation. Although *ios1-1* has an ABA-hypersensitive-like phenotype, susceptibility to downy mildew is less strongly reduced in *ios1-1* than in *abh1*. We previously showed that IOS1 is encoded by a gene that gave rise to a cluster of 11 IOS1-like MLD-RLKs through successive gene duplications (Hok et al., 2011). Three other genes from the cluster were found to be coregulated with *IOS1* during downy mildew infection (Hok et al., 2011). The weaker interaction phenotype of the *ios1-1* mutant, when compared with *abh1*, might reflect that other members of the cluster participate in the down-regulation of ABA signaling and cooperate in disease promotion.

The oomycete pathogens studied here sporulate through stomata, and *P. parasitica* also employs stomata to reenter leaf tissues (Supplemental Fig. S8). Increasing stomatal opening due to a down-regulation of ABA signaling would thus favor the entry and exit of these pathogens. However, powdery mildew infection is largely independent of stomatal opening, as the fungus feeds on epidermal cells and does not enter the leaf tissue. Furthermore, IOS1 appears to play a predominant role during the early stages of infection, whereas the sporulation of *Hpa* through open stomata characterizes the end of the disease cycle. Induced stomatal opening might thus favor other parameters affecting biotrophic infection, such as the increase in transpiration and water loss from leaf cells. The resulting decrease in leaf cell turgor pressure might induce phloem cells with a higher turgor pressure to discharge their metabolites into the leaf cells, which would potentially become sinks for nutrients that might then become available to the feeding structures of biotrophic pathogens. Independent of the effects on stomata, ABA influences stress responses as well as the aging of plant tissues (Lim et al., 2007). IOS1-mediated down-regulation of ABA signaling results in the activation of *COR* and *RD* gene expression. These genes are transiently expressed during the cooling responses of Arabidopsis (Wang and Hua, 2009), which we likely induced in our experimental setup, and are also expressed during the senescence of plant tissues (Yang et al., 2011). The down-regulation of *COR/RD* genes upon infection might thus indicate that biotrophs attenuate stress-associated senescence programs of the host cells for successful infection.

ABA also interferes with signaling pathways involving the defense hormones SA, JA, and ethylene. One would expect that an interference of IOS1 with defense hormone signaling upon *Hpa* infection would influence the expression of defense-related genes that are controlled by these hormones. However, the conventional marker genes *PR1a*, *PR4*, and *PDF1.2* were not more responsive in *ios1-1* upon *Hpa* infection when compared with the wild type. By contrast, genes encoding the defense regulators WRKY33, WRKY70, and PAD4 were up-regulated to some extent in *ios1-1* at the early stages of infection. WRKY33 seems also to be involved in the regulation of thermotolerance (Li et al., 2011), and WRKY70 was recently described as a negative regulator of stomatal closure and osmotic stress tolerance in Arabidopsis (Li et al., 2013). PAD4 is essential in effector-triggered immune signaling, but it is also required for the down-regulation of ABA signaling (Kim et al., 2011). These genes are thus involved both in defense and in the negative regulation of ABA signaling. Their activation in *ios1-1* might reflect the existence of a feedback loop, which counteracts excessive ABA signaling. We cannot exclude that a subtly nuanced cross talk between ABA and defense hormones contributes to

the observed interaction phenotypes of the *ios1-1* mutant. But taken together, our findings indicate a loss of susceptibility to (hemi)biotrophic filamentous pathogens rather than a gain of defense in plants that lack IOS1.

IOS1 appears to have a multifaceted role in the interaction of Arabidopsis with microbes, depending on the kind of infecting pathogen. Our findings determine IOS1 as a plant factor promoting infection by filamentous (hemi)biotrophs and as a negative regulatory element of ABA signaling. By contrast, IOS1 plays a critical role in the onset of PTI during the interaction of Arabidopsis with *P. syringae* (Chen et al., 2014). It associates with the recognition receptors for bacterial pathogen-associated molecular patterns, FLS2 and EFR, and their coreceptor BAK1. The absence of IOS1 in mutant plants confers an attenuated PTI response and increased susceptibility to the bacteria. In this interaction, IOS1 acts as a positive regulatory element in PTI upstream of mitogen-activated protein kinase signaling. Consequently, both the expression of PTI marker genes (such as *FRK1*) and callose deposition were attenuated in the absence of IOS1 upon bacterial perception. During the interaction with filamentous (hemi)biotrophs, however, IOS1 seems to be engaged in a PTI-independent signaling pathway, as we found that the induction of genes involved in early defense signaling (*FRK1*, *NHL10*, and *WRKY29*) upon *Hpa* infection and callose deposition in the interaction with powdery mildew did not change in *ios1-1* when compared with the wild-type plants. Chen et al. (2014) also found that IOS1 did not interfere with infection by the necrotrophic fungal pathogen *Botrytis cinerea*, further supporting a pathogen-dependent role of IOS1. It has to be noted that three allelic mutants, *ios1-1*, *ios1-2*, and *ios1-3*, are available. The mutant *ios1-1* is a full knockout, whereas both *ios1-2* and *ios1-3* produce transcripts that probably translate for IOS1 proteins with a truncated kinase domain (Chen et al., 2014; Supplemental Fig. S9). In the interaction with *P. syringae*, *ios1-1*, *ios1-2*, and *ios1-3* showed similar PTI defects, and it was also shown that IOS1 requires an active kinase for the association with FLS2 and BAK1 and for the concomitant activation of the PTI response after challenge with *P. syringae* (Chen et al., 2014). By contrast, signaling is probably independent of the IOS1 kinase activity upon infection with *Hpa*, because in our hands only *ios1-1*, but not *ios1-2* or *ios1-3*, was hypersensitive to ABA and more resistant to *Hpa* (data not shown). We suppose that IOS1 may associate with other protein(s) that ensure(s) the downstream signaling events during the interaction with *Hpa* and other filamentous (hemi)biotrophs, independent of the intrinsic IOS1 kinase domain. Interestingly, a recent large-scale analysis of the membrane protein interactome of Arabidopsis indicated that IOS1 interacts with a PP2C (Jones et al., 2014) that belongs to the ABI1-related PP2C family (Schweighofer et al., 2004). This finding requires confirmation, but it may indicate that IOS1 down-regulates ABA signaling at the PP2C node, where the ABA signal is transduced through the inhibition of PP2Cs by activated PYR/PYL/RCAR receptors (Cutler et al., 2010). The same screen revealed CRK50, a Cys-rich RLK, as another protein that potentially interacts with IOS1 (Jones et al., 2014). This may further support that IOS1 employs different modes of signaling for the activation of PTI in the interaction with *P. syringae* and for the down-regulation of ABA upon infection with *Hpa*.

MLD-RLKs constitute a large protein family in Arabidopsis, but functional data have only recently become available for some of the family members. The MLD-RLKs described to date control several processes involved in reproduction. MLD-RLKs from the OUTGROWTH-ASSOCIATED PROTEIN KINASE cluster control the combination quality of intraspecific hybrids after fertilization (Smith et al., 2011). THESEUS1 and HERKULES1 govern cell elongation in flower stalks (Guo et al., 2009). ANXUR (ANX1 and ANX2) and FER coordinate the behavior of male and female reproductive organs, respectively, during pollen tube perception in fertilization (Boisson-Dernier et al., 2009; Miyazaki et al., 2009). FER is responsible for egg cell polarization, and *fer* mutants are particularly resistant to powdery mildew fungi (Kessler et al., 2010). FER has recently been shown to down-regulate ABA signaling (Yu et al., 2012), and it has been suggested that tip-growing hyphae from the fungus resemble progressing pollen tubes (Kessler et al., 2010). In this scenario, the hyphae make use of FER, as a conserved component, to polarize host cells before establishing haustoria and to down-regulate ABA signaling to facilitate disease progression. The functional analogy of IOS1 with FER (negative regulation of ABA signaling), and its structural similarity with SYMRK, suggest that IOS1 is one of the conserved elements that evolved in plants for the detection of beneficial filaments and that may have since been exploited by pathogens for the establishment of disease.

In conclusion, we show that IOS1 negatively regulates ABA signaling and that an absence of the MLD-RLK confers ABA hypersensitivity to Arabidopsis. Our findings strongly suggest that mildews exploit the receptor to down-regulate ABA signaling in the host upon infection. IOS1 thus appears to pivot the outcome of interactions between Arabidopsis and the biotic environment, as it both primes PTI to *P. syringae* and supports the infection success of filamentous biotrophs.

MATERIALS AND METHODS

Plant Material

The Arabidopsis (*Arabidopsis thaliana*) mutants *ios1-1* (Hok et al., 2011), *abh1* (Hugouvieux et al., 2001), and *abi1-1* (Koornneef et al., 1984) and the complemented *ios1-1cp4* line (Hok et al., 2011) have been described. A line harboring the *pRD29B::GUS* reporter (Christmann et al., 2005) in the Landsberg *erecta* background was crossed with *ios1-1*, and lines homozygous for both the mutation and the reporter transgene were used for analysis.

Plant Growth Conditions and Treatments

If not stated otherwise, plants were grown in growth cabinets at 20°C with a 12-h photoperiod (Hok et al., 2011). For germination assays, seeds were sown on Gamborg's B5 medium including vitamins (Duchefa), which was complemented with 1% (w/v) Suc and ABA (±racemate containing 50% [w/v]

active ABA; Sigma-Aldrich A1049). For growth assays, seeds were sown without ABA and transferred to medium containing 10 μM (±)-ABA 1 week later. Root elongation was measured from this time point. Alternatively, 1-week-old plantlets from the reporter line were transferred to medium containing Fluridon (Sigma-Aldrich 45511). The responsiveness of *COR* genes to exogenous ABA application was analyzed after spraying water or (±)-ABA at 0.5 and 5 μM onto 8-d-old seedlings and further incubation at 20°C in the light in a water-saturated atmosphere. To analyze the influence of exogenously applied ABA on the interaction with *Hyaloperonospora arabidopsidis*, 7-d-old seedlings were sprayed twice with water or 10 μM (±)-ABA 6 h prior to inoculation and 24 h after inoculation with conidiospores. To stimulate RD29B expression, plants were sprayed with a solution containing 10 μM (±)-ABA, 0.1% (v/v) dimethyl sulfoxide, and 0.005% (v/v) Silwett 1 d after inoculation with *Hpa* or treatment with water. Alternatively, plants inoculated or not with *Hpa* were placed in a Superdry SD 302-21 cabinet (Totech) at 15% relative humidity 2 d after inoculation.

Pathogen Assays

Interaction studies with *Hpa* and *Phytophthora parasitica* were performed and analyzed according to Hok et al. (2011) and Attard et al. (2010), respectively. Conidia from *Erysiphe cruciferarum* were sprayed on 5-week-old plants at an inoculation density of 3 to 5 conidia mm^{-2}. Powdery mildew symptoms were examined 7 d after inoculation. For conidiophore production, leaves were fixed 5 d after inoculation, and fungal structures were stained with acetic ink (Hoefle et al., 2011). Inoculations with *Ralstonia solanacearum* strain GMI1000, and the scoring of disease symptoms, were performed according to Hirsch et al. (2002).

Determination of ABA Concentrations in Plant Tissues

Lyophilized plant material (100 mg fresh weight equivalent per sample) was homogenized. Each sample was analyzed as two technical and three biological replicates. [$^2H_6$]ABA was supplied by the Plant Biotechnology Institute, National Research Council of Canada. Further sample preparation was performed according to Meixner et al. (2005) with some modifications. After centrifugation of the samples at 10,000*g* for 10 min, the supernatant was removed and evaporated to dryness under a stream of N_2. The residue was resuspended in 200 μL of methanol and centrifuged again under the same conditions, and the supernatant was removed and placed in a glass vial. The methanol was evaporated under a stream of N_2, and the sample was resuspended in methanol. Methylation was performed by adding equal sample amounts of a 1:10 diluted solution (in diethylether) of trimethylsilyldiazomethane solution (Sigma-Aldrich) for 30 min at room temperature. The mixture was then evaporated and resuspended in 50 μL of ethyl acetate for gas chromatography-mass spectrometry analysis.

Gas chromatography-mass spectrometry analysis was carried out on a Varian Saturn 2100 ion-trap mass spectrometer, using electron-impact ionization at 70 eV, connected to a Varian CP-3900 gas chromatograph equipped with a CP-8400 autosampler (Varian). For the analysis, 1 μL of the methylated sample was injected in the splitless mode (splitter opening 1:100 after 1 min) onto a Phenomenex ZB-5 column (30 m × 0.25 mm × 0.25 μm) using helium carrier gas at 1 mL min^{-1}. Injector temperature was 250°C, and the temperature program was 60°C for 1 min, followed by an increase of 25°C min^{-1} to 180°C, 5°C min^{-1} to 250°C, 25°C min^{-1} to 280°C, and then 5 min isothermically at 280°C. For higher sensitivity, the μSIS mode (Varian manual; Wells and Huston, 1995) was used. The endogenous hormone concentrations were calculated by the principles of isotope dilution (at mass-to-charge ratio 190/194 [endogenous and labeled standard]; note that during fragmentation of ABA, two deuteriums are lost) for methylated ABA (Walker-Simmons et al., 2000).

Detection of Reporter Gene Expression

Samples were analyzed by confocal microscopy for fluorescence of the GFP reporter. GUS activity was stained histochemically with 5-bromo-4-chloro-3-indolyl-β-glucuronic acid (Eurogentec) and analyzed with an Axioplan 2 microscope (Carl Zeiss) using transmission light optics. For localization in thin-sectioned tissues, 5-bromo-4-chloro-3-indolyl-β-glucuronic acid-stained cotyledons were fixed in 2% (v/v) glutaraldehyde in 50 mM PIPES, pH 6.9, dehydrated, and embedded in Technovit 7100 (Heraeus Kulzer) as described by the manufacturer. Embedded tissues were sectioned (6 μm) and mounted in Depex (Sigma-Aldrich). Microscopy was performed on the Zeiss Axioplan 2 microscope using dark-field optics. In vitro GUS activity was determined through the enzymatic conversion of 4-methylumbelliferyl-glucuronide (Jefferson et al., 1987). The fluorescence of generated methylumbelliferone was determined with an automated Xenius fluorimeter (SAFAS) under continuous agitation (600 V; excitation, 350 nm; emission, 450 nm; bandwith, 10 nm). Specific enzymatic activity was calculated according to a calibration curve established with commercial methylumbelliferone (Sigma-Aldrich).

Confocal Microscopy

Optical sections were obtained using an inverted confocal microscope (model LSM 510 META; Carl Zeiss) equipped with an argon ion and helium-neon laser as excitation source. GFP fluorescence emission in samples was detected after excitation at 488 nm through a 505- to 530-nm band-pass emission filter.

Reverse Transcription-PCR

RNA was extracted from 50 mg of seedlings with the Isolate II RNA Plant Kit (Bioline). Reverse transcription, quantitative PCR, and data analysis were performed according to Hok et al. (2011). For primer sequences, see Supplemental Table S1.

Thermography

Plants were grown for 4 weeks at 20°C with an 8-h photoperiod. Before thermography, plants were exposed for 48 h to continuous light at room temperature under low relative humidity. In three experimental repetitions, infrared recordings were performed with a Thermacam PM250 (Inframetrics, FLIR Systems) on at least 20 positions per rosette for eight different plants per line.

Measurement of Stomatal Density, Aperture, and Conductance

Epidermal peels of leaves from 4-week-old plants were prepared on a microscope slide with medical adhesive Telesis V (Premiere Products). Stomata were allowed to close for 2.5 h in the dark in a medium containing 10 mM MES, 10 mM KCl, and 7.5 mM iminodiacetic acid at pH 6.2 and were then either incubated for 3 h in white light in the same medium containing 50 μM (±)-ABA or kept in the dark for 3 h after the addition of 10 μM glibenclamide (Enzo Life Sciences). All peels were analyzed with an Axioplan 2 microscope equipped with an Axiocam camera (Carl Zeiss). Stomatal density and aperture were determined with the Zeiss Axiovision digital image-processing software, version 4.4. Stomatal conductance was measured with leaves of 6-week-old short-day-grown plants using a GFS-3000 infrared gas analyzer (Walz). Assimilation rate, transpiration rate, and stomatal conductance were calculated using the GFSwin version 2.0 software (Walz). To analyze ABA-dependent stomatal closure, leaves were detached, transferred to 2 mL of water, and adapted for 10 min to light (200 μE m^{-2} s^{-1}), temperature (22°C), and CO_2 (350 μL L^{-1}). Petioles were then transferred to different ABA concentrations, and gas exchange was recorded in a 3-cm^2 cell at 200 μE m^{-2} s^{-1}, 22°C, and 13,000 μL L^{-1} water (56% relative humidity) until stomatal aperture reached steady state at about 25 to 40 min after transfer. To increase reproducibility, measurements were conducted only during the first half of the light period.

Sequence data from this article, and details for Arabidopsis loci, can be found at the GenBank/EMBL data libraries and The Arabidopsis Information Resource under accession numbers At1g51800 (*IOS1*), At2g19190 (*FRK1*), At2g35980 (*NHL10*), At2g38470 (*WRKY33*), At3g52430 (*PAD4*), At2g14610 (*PR1a*), At2g26020 (*PDF1-2*), At3g04720 (*PR4*), At4g23550 (*WRKY29*), At3g56400 (*WRKY70*), At5g52310 (*RD29A*), At5g52300 (*RD29B*), At2g42530 (*COR15B*), At2g42540 (*COR15A*), At5g10790 (*UBIQUITIN-SPECIFIC PROTEASE22*), At5g11770 (*NADH-UBIQUINONE OXIDOREDUCTASE 20 kD SUBUNIT*), and At5g62050 (*HOMOLOG OF YEAST OXIDASE ASSEMBLY1*).

Supplemental Data

The following materials are available in the online version of this article.

Supplemental Figure S1. IOS1 affects powdery mildew disease but not bacterial wilt.

Supplemental Figure S2. *ios1-1* mutants have no aberrant developmental phenotypes.

Supplemental Figure S3. The *ios1-1* mutation does not affect callose deposition in powdery mildew-infected leaves.

Supplemental Figure S4. ABA does not induce *IOS1* expression.

Supplemental Figure S5. ABA levels in cotyledons from Arabidopsis plants.

Supplemental Figure S6. ABA-induced, transient expression of *COR* genes is accelerated in the *ios1-1* mutant.

Supplemental Figure S7. ABA-sensitive reporter gene expression is down-regulated in *Hpa*-inoculated wild-type plants but not in *ios1-1*.

Supplemental Figure S8. Proposed role of IOS1 during infection with filamentous (hemi)biotrophs.

Supplemental Figure S9. Transcripts produced by *ios1* mutants.

Supplemental Table S1. Accession numbers, names, and primer sequences for genes analyzed in this study.

ACKNOWLEDGMENTS

We thank Nathalie Leonhardt (Commissariat à l'Energie Atomique) for providing the *abh1* and *abi1-1* mutants and Moritz Ruschhaupt (Technical University Munich) for communicating unpublished primer sequences.

Received August 12, 2014; accepted September 30, 2014; published October 1, 2014.

LITERATURE CITED

Albrecht C, Boutrot F, Segonzac C, Schwessinger B, Gimenez-Ibanez S, Chinchilla D, Rathjen JP, de Vries SC, Zipfel C (2012) Brassinosteroids inhibit pathogen-associated molecular pattern-triggered immune signaling independent of the receptor kinase BAK1. Proc Natl Acad Sci USA **109:** 303–308

Asai T, Tena G, Plotnikova J, Willmann MR, Chiu WL, Gomez-Gomez L, Boller T, Ausubel FM, Sheen J (2002) MAP kinase signalling cascade in Arabidopsis innate immunity. Nature **415:** 977–983

Attard A, Gourgues M, Callemeyn-Torre N, Keller H (2010) The immediate activation of defense responses in *Arabidopsis* roots is not sufficient to prevent *Phytophthora parasitica* infection. New Phytol **187:** 449–460

Bai L, Zhang G, Zhou Y, Zhang Z, Wang W, Du Y, Wu Z, Song CP (2009) Plasma membrane-associated proline-rich extensin-like receptor kinase 4, a novel regulator of Ca signalling, is required for abscisic acid responses in Arabidopsis thaliana. Plant J **60:** 314–327

Belkhadir Y, Jaillais Y, Epple P, Balsemão-Pires E, Dangl JL, Chory J (2012) Brassinosteroids modulate the efficiency of plant immune responses to microbe-associated molecular patterns. Proc Natl Acad Sci USA **109:** 297–302

Birkenbihl RP, Diezel C, Somssich IE (2012) Arabidopsis WRKY33 is a key transcriptional regulator of hormonal and metabolic responses toward *Botrytis cinerea* infection. Plant Physiol **159:** 266–285

Boisson-Dernier A, Roy S, Kritsas K, Grobei MA, Jaciubek M, Schroeder JI, Grossniklaus U (2009) Disruption of the pollen-expressed FERONIA homologs ANXUR1 and ANXUR2 triggers pollen tube discharge. Development **136:** 3279–3288

Boudsocq M, Willmann MR, McCormack M, Lee H, Shan L, He P, Bush J, Cheng SH, Sheen J (2010) Differential innate immune signalling via Ca^{2+} sensor protein kinases. Nature **464:** 418–422

Capoen W, Goormachtig S, De Rycke R, Schroeyers K, Holsters M (2005) SrSymRK, a plant receptor essential for symbiosome formation. Proc Natl Acad Sci USA **102:** 10369–10374

Chen CW, Panzeri D, Yeh YH, Kadota Y, Huang PY, Tao CN, Roux M, Chien SC, Chin TC, Chu PW, et al (2014) The *Arabidopsis* malectin-like leucine-rich repeat receptor-like kinase IOS1 associates with the pattern recognition receptors FLS2 and EFR and is critical for priming of pattern-triggered immunity. Plant Cell **26:** 3201–3219

Chen Y, Hu D, Yabe R, Tateno H, Qin SY, Matsumoto N, Hirabayashi J, Yamamoto K (2011) Role of malectin in $Glc_2Man_9GlcNAc_2$-dependent quality control of α1-antitrypsin. Mol Biol Cell **22:** 3559–3570

Chinchilla D, Shan L, He P, de Vries S, Kemmerling B (2009) One for all: the receptor-associated kinase BAK1. Trends Plant Sci **14:** 535–541

Christmann A, Hoffmann T, Teplova I, Grill E, Müller A (2005) Generation of active pools of abscisic acid revealed by in vivo imaging of water-stressed Arabidopsis. Plant Physiol **137:** 209–219

Cutler SR, Rodriguez PL, Finkelstein RR, Abrams SR (2010) Abscisic acid: emergence of a core signaling network. Annu Rev Plant Biol **61:** 651–679

de Torres-Zabala M, Truman W, Bennett MH, Lafforgue G, Mansfield JW, Rodriguez Egea P, Bögre L, Grant M (2007) *Pseudomonas syringae* pv. *tomato* hijacks the *Arabidopsis* abscisic acid signalling pathway to cause disease. EMBO J **26:** 1434–1443

Ellinger D, Naumann M, Falter C, Zwikowics C, Jamrow T, Manisseri C, Somerville SC, Voigt CA (2013) Elevated early callose deposition results in complete penetration resistance to powdery mildew in Arabidopsis. Plant Physiol **161:** 1433–1444

Glazebrook J (2005) Contrasting mechanisms of defense against biotrophic and necrotrophic pathogens. Annu Rev Phytopathol **43:** 205–227

Guo H, Li L, Ye H, Yu X, Algreen A, Yin Y (2009) Three related receptor-like kinases are required for optimal cell elongation in *Arabidopsis thaliana*. Proc Natl Acad Sci USA **106:** 7648–7653

Guo Y, Xiong L, Song CP, Gong D, Halfter U, Zhu JK (2002) A calcium sensor and its interacting protein kinase are global regulators of abscisic acid signaling in *Arabidopsis*. Dev Cell **3:** 233–244

He P, Shan L, Lin NC, Martin GB, Kemmerling B, Nürnberger T, Sheen J (2006) Specific bacterial suppressors of MAMP signaling upstream of MAPKKK in *Arabidopsis* innate immunity. Cell **125:** 563–575

Hirsch J, Deslandes L, Feng DX, Balagué C, Marco Y (2002) Delayed symptom development in *ein2-1*, an *Arabidopsis* ethylene-insensitive mutant, in response to bacterial wilt caused by *Ralstonia solanacearum*. Phytopathology **92:** 1142–1148

Hoefle C, Huesmann C, Schultheiss H, Börnke F, Hensel G, Kumlehn J, Hückelhoven R (2011) A barley ROP GTPase ACTIVATING PROTEIN associates with microtubules and regulates entry of the barley powdery mildew fungus into leaf epidermal cells. Plant Cell **23:** 2422–2439

Hok S, Danchin EG, Allasia V, Panabières F, Attard A, Keller H (2011) An *Arabidopsis* (malectin-like) leucine-rich repeat receptor-like kinase contributes to downy mildew disease. Plant Cell Environ **34:** 1944–1957

Hua J, Meyerowitz EM (1998) Ethylene responses are negatively regulated by a receptor gene family in *Arabidopsis thaliana*. Cell **94:** 261–271

Hugouvieux V, Kwak JM, Schroeder JI (2001) An mRNA cap binding protein, ABH1, modulates early abscisic acid signal transduction in *Arabidopsis*. Cell **106:** 477–487

Igarashi D, Tsuda K, Katagiri F (2012) The peptide growth factor, phytosulfokine, attenuates pattern-triggered immunity. Plant J **71:** 194–204

Inoue T, Higuchi M, Hashimoto Y, Seki M, Kobayashi M, Kato T, Tabata S, Shinozaki K, Kakimoto T (2001) Identification of CRE1 as a cytokinin receptor from *Arabidopsis*. Nature **409:** 1060–1063

Jefferson RA, Kavanagh TA, Bevan MW (1987) GUS fusions: beta-glucuronidase as a sensitive and versatile gene fusion marker in higher plants. EMBO J **6:** 3901–3907

Jones AM, Xuan Y, Xu M, Wang RS, Ho CH, Lalonde S, You CH, Sardi MI, Parsa SA, Smith-Valle E, et al (2014) Border control: a membrane-linked interactome of Arabidopsis. Science **344:** 711–716

Jones HG (1999) Use of thermography for quantitative studies of spatial and temporal variation of stomatal conductance over leaf surfaces. Plant Cell Environ **22:** 1043–1055

Kessler SA, Shimosato-Asano H, Keinath NF, Wuest SE, Ingram G, Panstruga R, Grossniklaus U (2010) Conserved molecular components for pollen tube reception and fungal invasion. Science **330:** 968–971

Kim TH, Hauser F, Ha T, Xue S, Böhmer M, Nishimura N, Munemasa S, Hubbard K, Peine N, Lee BH, et al (2011) Chemical genetics reveals negative regulation of abscisic acid signaling by a plant immune response pathway. Curr Biol **21:** 990–997

Koornneef M, Reuling G, Karssen CM (1984) The isolation and characterization of abscisic acid-insensitive mutants of *Arabidopsis thaliana*. Physiol Plant **61:** 377–383

Kosuta S, Held M, Hossain MS, Morieri G, Macgillivary A, Johansen C, Antolín-Llovera M, Parniske M, Oldroyd GE, Downie AJ, et al (2011) *Lotus japonicus symRK-14* uncouples the cortical and epidermal symbiotic program. Plant J **67:** 929–940

Leonhardt N, Vavasseur A, Forestier C (1999) ATP binding cassette modulators control abscisic acid-regulated slow anion channels in guard cells. Plant Cell **11:** 1141–1152

Li J, Besseau S, Törönen P, Sipari N, Kollist H, Holm L, Palva ET (2013) Defense-related transcription factors WRKY70 and WRKY54 modulate osmotic stress tolerance by regulating stomatal aperture in *Arabidopsis*. New Phytol **200:** 457–472

Li J, Brader G, Kariola T, Palva ET (2006) WRKY70 modulates the selection of signaling pathways in plant defense. Plant J **46:** 477–491

Li S, Fu Q, Chen L, Huang W, Yu D (2011) *Arabidopsis thaliana* WRKY25, WRKY26, and WRKY33 coordinate induction of plant thermotolerance. Planta **233:** 1237–1252

Lim PO, Kim HJ, Nam HG (2007) Leaf senescence. Annu Rev Plant Biol **58:** 115–136

Lindner H, Müller LM, Boisson-Dernier A, Grossniklaus U (2012) CrRLK1L receptor-like kinases: not just another brick in the wall. Curr Opin Plant Biol **15:** 659–669

Liu X, Yue Y, Li B, Nie Y, Li W, Wu WH, Ma L (2007) A G protein-coupled receptor is a plasma membrane receptor for the plant hormone abscisic acid. Science **315:** 1712–1716

Markmann K, Giczey G, Parniske M (2008) Functional adaptation of a plant receptor-kinase paved the way for the evolution of intracellular root symbioses with bacteria. PLoS Biol **6:** e68

Matsubayashi Y, Ogawa M, Morita A, Sakagami Y (2002) An LRR receptor kinase involved in perception of a peptide plant hormone, phytosulfokine. Science **296:** 1470–1472

Meixner C, Ludwig-Müller J, Miersch O, Gresshoff P, Staehelin C, Vierheilig H (2005) Lack of mycorrhizal autoregulation and phytohormonal changes in the supernodulating soybean mutant *nts1007*. Planta **222:** 709–715

Meng X, Xu J, He Y, Yang KY, Mordorski B, Liu Y, Zhang S (2013) Phosphorylation of an ERF transcription factor by *Arabidopsis* MPK3/MPK6 regulates plant defense gene induction and fungal resistance. Plant Cell **25:** 1126–1142

Miyazaki S, Murata T, Sakurai-Ozato N, Kubo M, Demura T, Fukuda H, Hasebe M (2009) ANXUR1 and 2, sister genes to FERONIA/SIRENE, are male factors for coordinated fertilization. Curr Biol **19:** 1327–1331

Mohr PG, Cahill DM (2003) Abscisic acid influences the susceptibility of *Arabidopsis thaliana* to *Pseudomonas syringae* pv. *tomato* and *Peronospora parasitica*. Funct Plant Biol **30:** 461–469

Mosher S, Seybold H, Rodriguez P, Stahl M, Davies KA, Dayaratne S, Morillo SA, Wierzba M, Favery B, Keller H, et al (2013) The tyrosine-sulfated peptide receptors PSKR1 and PSY1R modify the immunity of *Arabidopsis* to biotrophic and necrotrophic pathogens in an antagonistic manner. Plant J **73:** 469–482

Motose H, Iwamoto K, Endo S, Demura T, Sakagami Y, Matsubayashi Y, Moore KL, Fukuda H (2009) Involvement of phytosulfokine in the attenuation of stress response during the transdifferentiation of zinnia mesophyll cells into tracheary elements. Plant Physiol **150:** 437–447

Mustilli AC, Merlot S, Vavasseur A, Fenzi F, Giraudat J (2002) *Arabidopsis* OST1 protein kinase mediates the regulation of stomatal aperture by abscisic acid and acts upstream of reactive oxygen species production. Plant Cell **14:** 3089–3099

Osakabe Y, Maruyama K, Seki M, Satou M, Shinozaki K, Yamaguchi-Shinozaki K (2005) Leucine-rich repeat receptor-like kinase1 is a key membrane-bound regulator of abscisic acid early signaling in *Arabidopsis*. Plant Cell **17:** 1105–1119

Robert-Seilaniantz A, Grant M, Jones JD (2011) Hormone crosstalk in plant disease and defense: more than just jasmonate-salicylate antagonism. Annu Rev Phytopathol **49:** 317–343

Schallus T, Jaeckh C, Fehér K, Palma AS, Liu Y, Simpson JC, Mackeen M, Stier G, Gibson TJ, Feizi T, et al (2008) Malectin: a novel carbohydrate-binding protein of the endoplasmic reticulum and a candidate player in the early steps of protein N-glycosylation. Mol Biol Cell **19:** 3404–3414

Schweighofer A, Hirt H, Meskiene I (2004) Plant PP2C phosphatases: emerging functions in stress signaling. Trends Plant Sci **9:** 236–243

Smith LM, Bomblies K, Weigel D (2011) Complex evolutionary events at a tandem cluster of *Arabidopsis thaliana* genes resulting in a single-locus genetic incompatibility. PLoS Genet **7:** e1002164

Stracke S, Kistner C, Yoshida S, Mulder L, Sato S, Kaneko T, Tabata S, Sandal N, Stougaard J, Szczyglowski K, et al (2002) A plant receptor-like kinase required for both bacterial and fungal symbiosis. Nature **417:** 959–962

Tan X, Calderon-Villalobos LI, Sharon M, Zheng C, Robinson CV, Estelle M, Zheng N (2007) Mechanism of auxin perception by the TIR1 ubiquitin ligase. Nature **446:** 640–645

Tanaka H, Osakabe Y, Katsura S, Mizuno S, Maruyama K, Kusakabe K, Mizoi J, Shinozaki K, Yamaguchi-Shinozaki K (2012) Abiotic stress-inducible receptor-like kinases negatively control ABA signaling in *Arabidopsis*. Plant J **70:** 599–613

Ton J, Flors V, Mauch-Mani B (2009) The multifaceted role of ABA in disease resistance. Trends Plant Sci **14:** 310–317

Ueguchi-Tanaka M, Ashikari M, Nakajima M, Itoh H, Katoh E, Kobayashi M, Chow TY, Hsing YI, Kitano H, Yamaguchi I, et al (2005) GIBBERELLIN INSENSITIVE DWARF1 encodes a soluble receptor for gibberellin. Nature **437:** 693–698

Uno Y, Furihata T, Abe H, Yoshida R, Shinozaki K, Yamaguchi-Shinozaki K (2000) *Arabidopsis* basic leucine zipper transcription factors involved in an abscisic acid-dependent signal transduction pathway under drought and high-salinity conditions. Proc Natl Acad Sci USA **97:** 11632–11637

Walker-Simmons MK, Rose PA, Hogge LR, Abrams SR (2000) Abscisic acid: ABA immunoassay and gas chromatography/mass spectrometry verification. Methods Mol Biol **141:** 33–47

Wang Y, Hua J (2009) A moderate decrease in temperature induces COR15a expression through the CBF signaling cascade and enhances freezing tolerance. Plant J **60:** 340–349

Wells G, Huston C (1995) High-resolution selected ion monitoring in a quadrupole ion trap mass spectrometer. Anal Chem **67:** 3650–3655

Wiermer M, Feys BJ, Parker JE (2005) Plant immunity: the EDS1 regulatory node. Curr Opin Plant Biol **8:** 383–389

Xin Z, Wang A, Yang G, Gao P, Zheng ZL (2009) The Arabidopsis A4 subfamily of lectin receptor kinases negatively regulates abscisic acid response in seed germination. Plant Physiol **149:** 434–444

Yang SD, Seo PJ, Yoon HK, Park CM (2011) The *Arabidopsis* NAC transcription factor VNI2 integrates abscisic acid signals into leaf senescence via the *COR/RD* genes. Plant Cell **23:** 2155–2168

Yu F, Qian L, Nibau C, Duan Q, Kita D, Levasseur K, Li X, Lu C, Li H, Hou C, et al (2012) FERONIA receptor kinase pathway suppresses abscisic acid signaling in *Arabidopsis* by activating ABI2 phosphatase. Proc Natl Acad Sci USA **109:** 14693–14698